

# Short Homodimeric and Heterodimeric Coiled Coils

He Dong and Jeffrey D. Hartgerink\*

Departments of Chemistry and Bioengineering, Rice University, 6100 Main Street,  
Mail Stop 60, Houston, Texas 77005

Received November 1, 2005; Revised Manuscript Received January 17, 2006

In this communication, we discuss the design, synthesis, and characterization of four peptides which are able to self-assemble into five different homo- and heterodimeric  $\alpha$ -helical coiled coils based on the pH of their environment. These peptides are very short, containing only 14 or 21 amino acids each, and illustrate the minimum requirements necessary to form dimeric coiled coils which are critical in a large number of biological and materials design applications.

Coiled coils are one of the most attractive model systems for protein design and folding studies because of their simplicity, regularity, and diversity in structure and oligomerization state.<sup>1,2</sup> They are found in structural proteins such as the intermediate filaments,<sup>3</sup> proteins involved in muscle contraction such as myosin,<sup>4</sup> and DNA recognition proteins such as GCN4.<sup>5</sup> In addition, coiled coils have been used in a large variety of synthetic systems including nanofibers,<sup>6</sup> self-replicating systems,<sup>7</sup> catalysts,<sup>8</sup> and biomaterials.<sup>9</sup> For both natural and synthetic systems, it is desirable to know the minimum size necessary to achieve dimerization. In this communication, we report on the shortest known homomeric and heteromeric coiled coil dimers, containing just 14 amino acids per peptide.

In coiled coil design, a seven-amino-acid repeat (a “heptad” whose amino acids are denoted from *a* to *g*) is found in which amino acids in the *a* and *d* positions are hydrophobic, typically leucine, isoleucine, or valine. Because seven amino acids make approximately two turns of an  $\alpha$ -helix, the *a* and *d* positions align along one face of the  $\alpha$ -helix, making it highly hydrophobic. Burying these hydrophobic faces is the primary driving force for self-assembly. Positions *e* and *g* of a coiled coil are typically charged residues such as glutamic acid and lysine. These positions flank the hydrophobic face and are often involved in the formation of intra- or interhelical salt bridges to provide additional stability or to help specify the orientation of the two interacting peptide chains with respect to one another. The alignment, specificity, and oligomerization state of a coiled coil, therefore, is primarily determined by the interactions between residues in the *a*, *d*, *e*, and *g* positions, which together make up the dimerization interface (Figure 1).

Studies attempting to improve the stability of coiled coils have utilized chain-length optimization showing that increase in chain length causes an increase in stability, but in a nonlinear pattern, and a minimum of three heptad repeating units are required to stabilize coiled coil structure for both homo- and heterodimeric coiled coils.<sup>10</sup> Recent studies have also demonstrated that the chain length affects the kinetic and thermodynamic constants of interaction.<sup>11</sup> Stability of coiled coils has also been increased by adding  $\alpha$ -helix-favoring amino acids,<sup>12</sup> end capping to reduce unfavorable ion–helix dipole interactions, modifying the hydrophobicity of residues in the coiled coil hydrophobic core,<sup>2,13</sup> designing cation– $\pi$  interactions that reside at the interface between helices,<sup>14</sup> and introducing intra- or

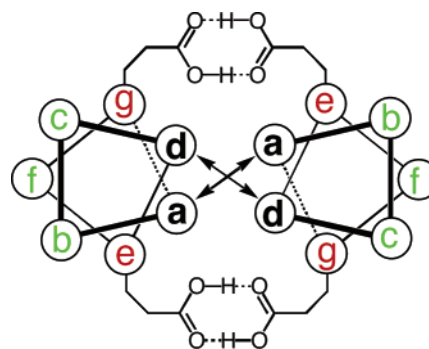


**Figure 1.** Schematic representation of dimeric  $\alpha$ -helical coiled coil highlighting the *a/d* hydrophobic packing and *e/g* hydrogen bonding.

**Table 1.** Peptide Primary Sequence

#	Sequence	mass <sup>a</sup> / mass <sup>b</sup>	oligomerization number
	<i>gabcdefgabcdefgabcdef<sup>c</sup></i>		
1	EIAQLLEYEISQLEQ	3300 / 1734	1.9
2	KIAQLKYKISQLKQ	1627 / 1730	0.9
3	EIAQLLEYEISQLEQEIQALES	5369 / 2505	2.1
4	KIQALKQKISQLKWKIQSLKQ	4916 / 2579	1.9

<sup>a</sup> Apparent molecular weight derived from AUC fitting to single-species model. <sup>b</sup> Calculated peptide monomeric mass. <sup>c</sup> Position in heptad. Red indicates negatively charged amino acids at pH 7; blue indicates positively charged amino acids at pH 7.

interhelical salt bridges by rational design.<sup>15</sup> Lustig has successfully designed the shortest known dimeric coiled coil peptide (15 amino acids in length) using a combination of the above design criteria.<sup>16</sup>

We designed and synthesized the peptides listed in Table 1 (for synthesis and characterization, see Supporting Information). All peptides were N-terminally acetylated and prepared with a C-terminal amide. Peptides utilized the hydrophobic amino acids isoleucine and leucine in the *a* and *d* positions, respectively, to form the hydrophobic core of the coiled coil and to favor parallel dimeric coiled coils.<sup>5,17</sup> Positions *e* and *g* consisted of glutamic acid in peptides 1 and 3 or lysine in the case of peptides 2 and 4 to allow pH-dependent self-assembly of homodimers or salt-bridged formation of heterodimeric mixtures of 1 with 2 and 3 with 4. It should be noted that because in all cases the amino acids in positions *e* and *g* are identical (both glutamic acid or both lysine) these interactions will be similar for both parallel and antiparallel coiled coils, although we expect a parallel

\* E-mail: jd@rice.edu.

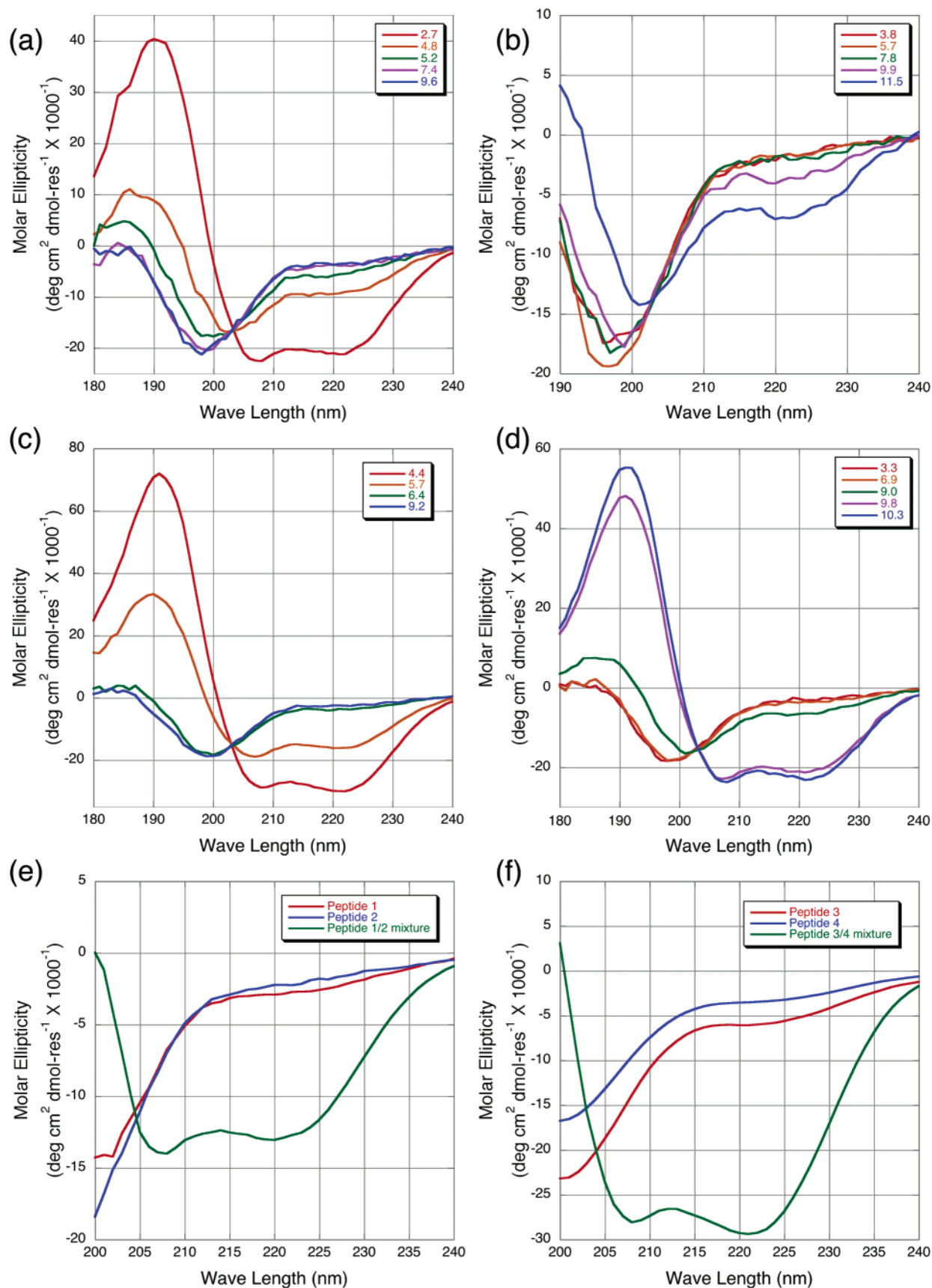


**Figure 2.** CD spectra of peptides 1–4 versus pH (a–d, respectively) showing the conversion from random to  $\alpha$ -helical structure. Mixtures of 1/2 and 3/4 (e and f, respectively) at neutral pH.

arrangement based on amino acid choice in *a* and *d* positions as represented in Figure 1. Heptad positions *b*, *c*, and *f* were filled with hydrophilic amino acids such as serine or glutamine,

the  $\alpha$ -helix-promoting amino acid alanine, or amino acids used to aid spectroscopic characterization such as tyrosine and tryptophan. Peptides **1** and **2** contained only 14 amino acids (2

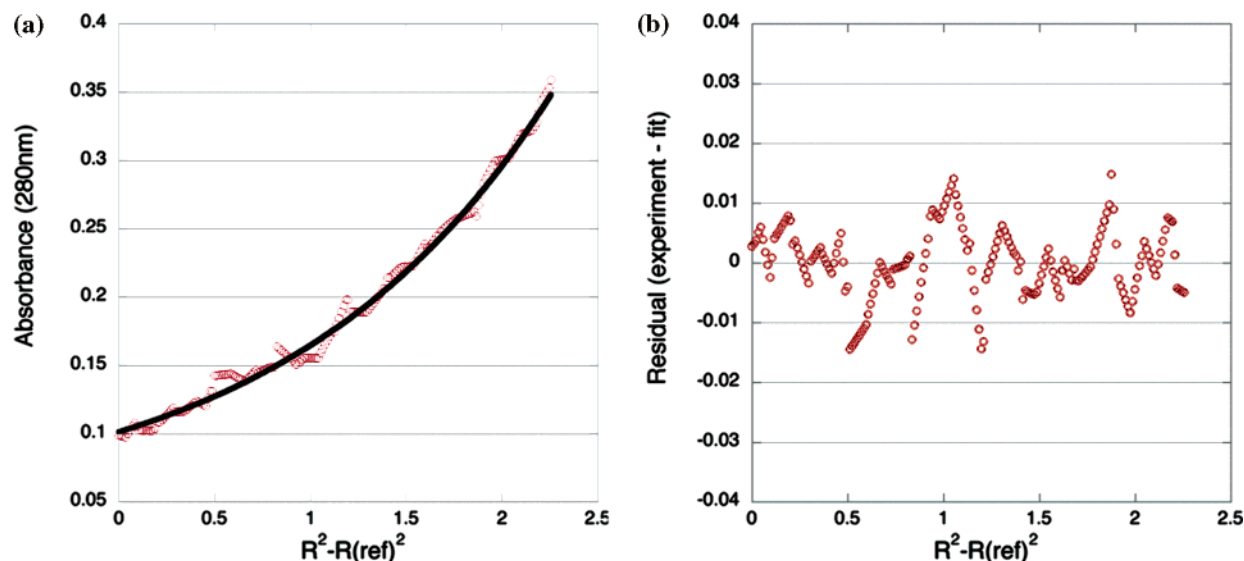


**Figure 3.** Representative sedimentation equilibrium data for peptide 1, 0.17 mM, pH 3, 55 000 rpm: (a) fitted (black curve) and experimental (red circle) overlay, (b) randomly distributed residual showing the validity of single-component model for evaluation. Experiments were run at three different concentrations and three different rotor speeds in phosphate buffer at 5 °C. Data were fit to single-component model yielding a molecular weight of 3300.

heptad repeats), while peptides **3** and **4** contained the same general amino acid sequence while containing 21 amino acids (3 heptad repeats). From these 4 peptides, a total of 5 coiled coils were prepared: 3 homodimeric and 2 heterodimeric.

Peptides **1** and **3** contain glutamic acid in all their *e* and *g* positions. At neutral pH, this leads to an overall net negative charge of  $-2$  per heptad. The ionic repulsion from this destabilizes the tightly wound  $\alpha$ -helix conformation and repels adjacent peptides at pHs above the  $pK_a$  of glutamic acid as indicated by circular dichroism spectroscopy (CD) (Figure 2a,c). Protonation of the side chains in an acidic environment eliminates the negative charges and also allows for the formation of favorable hydrogen bonds between glutamic acid side chains. Collectively, this allows the formation of  $\alpha$ -helical secondary structure with a calculated percent helicity of 65 for peptide **1** and 84 for peptide **3** using the method of Baldwin.<sup>18</sup> Analytical ultracentrifugation (AUC) indicates that both the 14-amino-acid and 21-amino-acid peptides self-assemble into homomeric coiled coil dimers when they are  $\alpha$ -helical at acidic pH (Figure 3 and Figures 6 and 8 in the Supporting Information).

In contrast, peptides **2** and **4** contain lysine in all their *e* and *g* positions, but are otherwise closely related to peptides **1** and **3**. These peptides are positively charged at neutral pH, which results in their disordered structure (Figure 2b,d). Neutralization of the repulsive positive charge leads to the formation of an  $\alpha$ -helical secondary structure in the case of peptide **4** (65%  $\alpha$ -helix), but only very weak helicity in the shorter peptide **2** (21%  $\alpha$ -helix). AUC confirms that peptide **4** forms a homomeric coiled coil dimer, while peptide **2** remains monomeric (Figures 7 and 9 in Supporting Information). The reason peptide **1** is able to form an  $\alpha$ -helical coiled coil, while peptide **2** is not, is probably due to the quality of hydrogen bonding that is able to be formed between a pair of carboxylic acids as compared to a pair of primary amines. In the case of glutamic acid, two symmetric hydrogen bonds are able to be formed between each glutamic acid pair, whereas the amine of lysine is unable to achieve this highly favorable type of hydrogen bonding.

Although peptide **1** was able to form a coiled coil dimer, this conformation is not stable for long periods of time: At room temperature, it slowly converts to an amyloid-like  $\beta$ -sheet hydrogen bonded structure,<sup>19</sup> over a period of about a day,

characterized by a CD spectrum with a strong negative peak at 217 nm (Figure 4a). The transition from  $\alpha$ -helix to  $\beta$ -sheet is highly dependent on temperature (Figure 4c). Below 15 °C, the coiled coil is stable for longer than a week, while above 40 °C, it converts to a  $\beta$ -sheet secondary structure in minutes. FT-IR of the amide I band confirms this structural transition showing a shift from  $1650\text{ cm}^{-1}$  to  $1626\text{ cm}^{-1}$  and  $1611\text{ cm}^{-1}$  (Figure 4d). Upon conversion to  $\beta$ -sheet secondary structure, the peptide is no longer soluble and precipitates from solution. The precipitate formed was characterized by congo-red-stained polarized light microscopy and displays the characteristic green/yellow birefringence associated with amyloid-like proteins (Figure 5a).<sup>20</sup> Examination of this precipitate by negative-stain TEM revealed nanofibers 4–5 nm in diameter (Figure 5b) corresponding to the expected length of the peptide in a fully extended conformation. This is consistent with the current understanding of amyloid nanofiber structure in which the peptide backbone is perpendicular to the nanofiber axis and an extensive  $\beta$ -sheet hydrogen bonding network is parallel to the nanofiber axis.<sup>21</sup>

In contrast, the longer peptides **3** and **4** are completely stable  $\alpha$ -helical coiled coil dimers and do not undergo a conformational change to a  $\beta$ -sheet structure. Peptide **3** forms a highly stable structure with 84% helicity as indicated by CD (Figure 2c). Denaturing experiments with this peptide show that 12 M guanidinium hydrochloride and heating is needed to fully unfold this structure (Supporting Information Figure 5). Peptide **4** forms with a helicity of 65%, again showing the less favorable interactions able to be achieved by lysine-containing peptides.

Peptides **1**, **3**, and **4** each formed homomeric coiled coil dimers at pHs in which their ionizable side chains were neutralized as characterized by AUC and CD and in all cases were disorganized at neutral pH. However, at neutral pH, equal molar mixtures of peptides **1** with **2** and **3** with **4** also form  $\alpha$ -helices. A heterodimeric coiled coil consisting of peptides **3** and **4** showed good  $\alpha$ -helical character by CD (83% helicity). The dimeric oligomerization state was confirmed by AUC (Supporting Information Figure 10), which yielded a mass of 5297. The mixture of peptide **1** with **2** showed significantly less helical character by CD and could not be characterized by AUC, because it rapidly converts to a  $\beta$ -sheet structure, similar

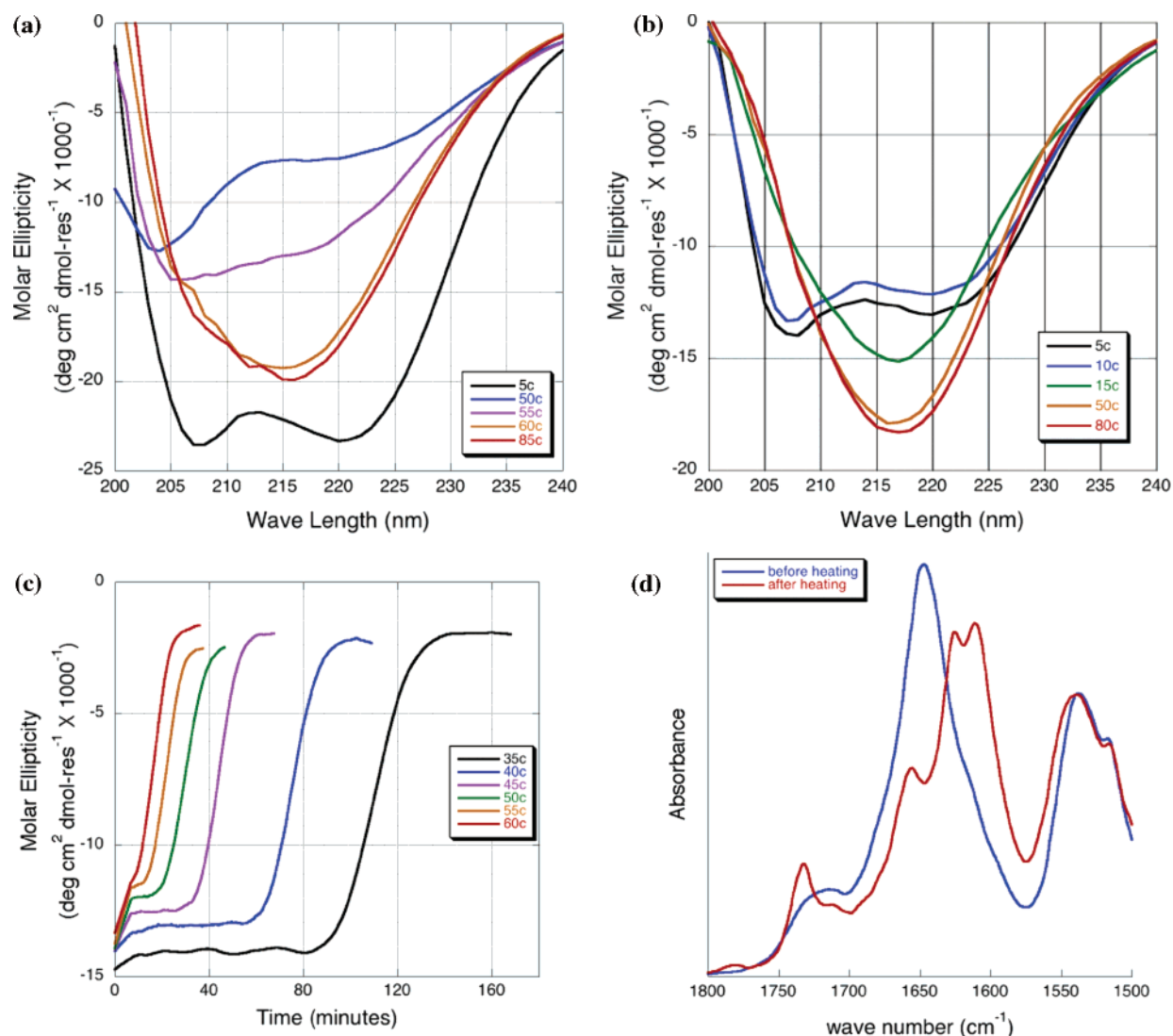


**Figure 4.** CD and IR data showing the conversion from  $\alpha$ -helical to  $\beta$ -sheet secondary structure. (a) CD of peptide **1** from low to high temperature. (b) CD peptide of a mixture of peptides **1** and **2** from low to high temperature. (c) CD of peptide **1** at 205 nm showing temperature-dependent transition to  $\beta$ -sheet secondary structure. (d) FT-IR of peptide **1** before and after heating to induce structural change.

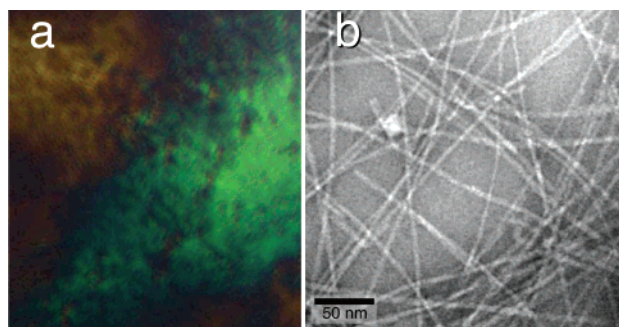


**Figure 5.** Polarized light microscopy and TEM. (a) Peptide **1** after conversion to  $\beta$ -sheet, stained with congo red, displaying the characteristic yellow–green birefringence. (b) Negative stain TEM image of peptide **1** after change to  $\beta$ -sheet conformation.

to peptide **1**, even at low temperature (Figure 4b). However, the fact that peptides **1** and **2** individually have essentially no helical content at neutral pH but have significant helicity (39%) when mixed together (Figure 2e) indicates that an induced conformational change must take place when the peptides interact, most likely as a heterodimeric coiled coil.

Our design favors a two-stranded  $\alpha$ -helical coiled coil using the established rules for construction of coiled coils. Peptides

containing the same hydrophobic core residues differ in the length and the amino acid residues at *e* and *g* positions. All the peptides, except peptide **2**, form stable  $\alpha$ -helical coiled coil dimers under conditions investigated where charged amino acids are completely neutralized to avoid electrostatic repulsion or are able to form complimentary charged pairs, as shown by analytical ultracentrifugation fittings (Figure 3, Supporting Information Figures 6–10). The failure of peptide **2** to form coiled coils may be due to the poorer hydrogen bonding available between neutralized lysine side chains. Additionally, lysine has the highest flexibility among all the 20 naturally occurring amino acids, making it entropically less favorable to interact in a fixed conformation in a coiled coil.

The 3-heptad peptides have a nearly identical sequence to that of 2-heptad peptides but are an additional 7 amino acids in length. This additional length allows them to form 2 additional turns of  $\alpha$ -helix and helps to stabilize them. The additional stability can be readily explained by examining the hydrogen bonding potential in an  $\alpha$ -helix in which both the N-terminal turn and C-terminal turn are unable to satisfy all of their backbone hydrogen bonding potential (4 hydrogen bonds at each termini remain unsatisfied). This leaves the termini relatively less stable as compared to the center of the helix. This



predicament is clearly worse the shorter the helical peptide. For example, 8 of 28 possible backbone hydrogen bond donors and acceptors will be unsatisfied in a 2-heptad peptide as compared to 8 of 42 in a 3-heptad  $\alpha$ -helix. The instability caused by the unsatisfied hydrogen bonding at the termini of the 2-heptad peptides may drive the initially stable  $\alpha$ -helical structure into the more thermodynamically stable  $\beta$ -sheet where all the hydrogen bonds may be satisfied.

In conclusion, we have designed, synthesized, and characterized peptides which undergo a pH-controllable formation of dimeric  $\alpha$ -helical coiled coils containing only 14 or 21 amino acids each. Depending on the selection of charged amino acids in the *e* and *g* positions of the heptad, these may be assembled at acidic, neutral, or basic pH. The simplicity and short length of these peptides will make them useful in the study of protein folding and stability. In addition, the peptides which undergo a structural transition from  $\alpha$ -helix to  $\beta$ -sheet may aid in the understanding the mechanism of amyloid fiber formation in a variety of neurodegenerative diseases.

**Acknowledgment.** We are grateful for the support of the Welch Foundation, the NSF for NIRT grant no. EEC-0304097 and the DOD for MURI grant no. W911NF-04-01-0203. J.D.H. is a recipient of the Searle Scholar Award.

**Supporting Information Available.** Synthetic methods, HPLC and mass spectra analysis of peptides, AUC data, and denaturation data. This material is available free of charge via the Internet at <http://pubs.acs.org>.

## References and Notes

- (1) Hodges, R. S. *Biochem. Cell Biol.* **1996**, *74*, 133–154. Woolfson, D. N. *Adv. Prot. Chem.* **2005**, *70*, 79.
- (2) Litowski, J. R.; Hodges, R. S. *J. Biol. Chem.* **2002**, *277* (40), 37272–37279.
- (3) Cohen, C.; Parry, D. A. D. *Proteins* **1990**, *7* (1), 1–15.
- (4) Schwaiger, I.; Sattler, C.; Hostetter, D. R.; Rief, M. *Nat. Mater.* **2002**, *1*, 232–235.
- (5) Harbury, P. B.; Zhang, T.; Kim, P. S.; Alber, T. *Science* **1993**, *262*, 1401–1407.
- (6) Smith, A. M.; Acquah, S. F. A.; Bone, N.; Kroto, H. W.; Ryadnov, M. G.; Stevens, M. S. P.; Walton, D. R.; Woolfson, D. N. *Angew. Chem., Int. Ed.* **2005**, *44*, 325–328. Zhou, M.; Bentley, D.; Ghosh, I. *J. Am. Chem. Soc.* **2004**, *126*, 734–735. Pandya, M. J.; Spooner, G. M.; Sunde, M.; Thorpe, J. R.; Rodger, A.; Woolfson, D. N. *Biochemistry* **2000**, *39* (30), 8728–8734.
- (7) Lee, D. H.; Severin, K.; Yokobayashi, Y.; Ghadiri, M. R. *Nature (London)* **1997**, *390*, 591–594. Saghatelian, A.; Yokobayashi, Y.; Soltani, K.; Ghadiri, M. R. *Nature (London)* **2001**, *409*, 797–801.
- (8) Kennan, A. J.; Haridas, V.; Severin, K.; Lee, D. H.; Ghadiri, M. R. *J. Am. Chem. Soc.* **2001**, *123*, 1797–1803. Severin, K.; Lee, D. H.; Kennan, A. J.; Ghadiri, M. R. *Nature (London)* **1997**, *389*, 706–709.
- (9) Wang, C.; Stewark, R. J.; Kopecek, J. *Nature (London)* **1999**, *397* (6718), 417–420. Petka, W. A.; Harden, J. L.; McGrath, K. P.; Wirtz, D.; Tirrell, D. A. *Science* **1998**, *281*, 389.
- (10) Kwok, S. C.; Hodges, R. S. *Biopolymers* **2003**, *71* (3), 329–329. Kwok, S. C.; Hodges, R. S. *Biopolymers* **2004**, *76* (5), 378–390. Su, J. Y.; Hodges, R. S.; Kay, C. M. *Biochemistry* **1994**, *33*, 15501–15510. Litowski, J. R.; Hodges, R. S. *J. Pept. Res.* **2001**, *58* (6), 477–492.
- (11) DeCrescenzo, G.; Litowski, J. R.; Hodges, R. S.; O'Connor-McCourt, M. D. *Biochemistry* **2003**, *42*, 1754–1763.
- (12) Chakrabarty, A.; Baldwin, R. L. *Adv. Protein Chem.* **1995**, *46*, 141–176.
- (13) Bilgic, B.; Kumar, K. *Tetrahedron* **2002**, *58*, 4105–4112. Kwok, S. C.; Hodges, R. S. *J. Biol. Chem.* **2004**, *279* (20), 21576–21588. Tripet, B.; Wagschal, K.; Lavigne, P.; Mant, C. T.; Hodges, R. S. *J. Mol. Biol.* **2000**, *300*, 377–402. Schnarr, N. A.; Kennan, A. J. *J. Am. Chem. Soc.* **2001**, *123* (44), 11081–11082.
- (14) Sakurai, Y.; Mizuno, T.; Hiroaki, H.; Gohda, K.; Oku, J.-i.; Tanaka T. *Angew. Chem., Int. Ed.* **2005**, *44*, 6180–6183.
- (15) Burkhard, P.; Ivaninskii, S.; Lustig, A. *J. Mol. Biol.* **2002**, *318*, 901–910.
- (16) Burkhard, P.; Meier, M.; Lustig, A. *Protein Sci.* **2000**, *9*, 2294–2301.
- (17) Zhu, B.-Y.; Zhou, N. E.; Kay, C. M.; Hodges, R. *Protein Sci.* **1993**, *2*, 383–394.
- (18) Scholtz, J. M.; Qian, H.; York, E. J.; Stewart, J. M.; Baldwin, R. L. *Biopolymers* **1991**, *31*, 1463–1470.
- (19) Takahashi, Y.; Ueno, A.; Mihara, H. *ChemBioChem* **2001**, *2* (1), 75–79. Takahashi, Y.; Ueno, A.; Mihara, H. *Chem.—Eur. J.* **1998**, *4* (12), 2475–2483. Ding, F.; LaRocque, J. J.; Dokholyan, N. V. *J. Biol. Chem.* **2005**, *280* (48), 40235–40240.
- (20) Klunk, W. E.; Pettegrew, J. W.; Abraham, D. J. *J. Histochem. Cytochem.* **1989**, *37* (8), 1273–1281.
- (21) Makin, O. S.; Atkins, E.; Sikorski, P.; Johansson, J.; Serpell, L. C. *Proc. Natl. Acad. Sci. U.S.A.* **2005**, *102* (2), 315–320. Nelson, R.; Sawaya, M. R.; Balbirnie, M.; Madsen, A. Ø.; Riekel, C.; Grothe, R.; Eisenberg, D. *Nature (London)* **2005**, *435*, 773–778.

BM050833N